Studies of Gas-Particle Interactions in a Microgravity Flow Cell
NASA Contract NAG3-2705
Final Report

Michel Louge (PI)*
Sibley School of Mechanical and Aerospace Engineering

James Jenkins (Co-I)
Department of Theoretical and Applied Mechanics

Anthony Reeves
Department of Electrical and Computer Engineering

Cornell University
Ithaca, NY

March 30, 2007

1 Executive Summary

The objective of the SiGMA project ("Solids interacting with a Gas in a Microgravity Apparatus") was to bring unique microgravity experimental insight to the detailed interactions between a gas and dispersed particles. By informing recent theories for those interactions, this work was meant to benefit NASA's exploration objectives by elucidating In-Situ Resource Utilization (ISRU) processes involving gases and dispersed solids, and by providing practical as well as theoretical insight to a wide array of industrial applications based on gas-solid suspensions.

Conscious of the merits of this investigation, several leading oil, food, chemical, pharmaceutical and mining companies provided additional support through the International Fine Particle Research Institute (IFPRI). Unfortunately, NASA could not commit resources to complete this and other similar projects, which it had regrouped in the Granular Flow Module under development for the International Space Station (ISS) by the NASA-Glenn Research Center (GRC).

This research was made possible by the development of a unique axisymmetric Couette cell producing shearing flows of gas and agitated solids in the absence of gravitational accelerations (Figure 1).

*Author to whom correspondence should be addressed. e-mail: MYL3@cornell.edu. Telephone: +1 607 255 4193.

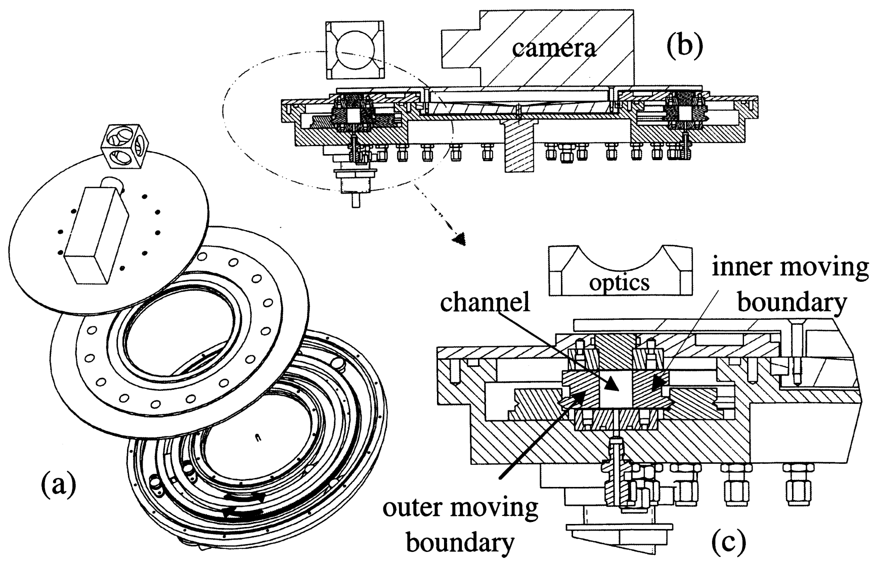

Figure 1: Conceptual sketch of the flight shear cell for the SiGMA project. (a) Exploded view showing possible counter-rotation of the inner and outer moving boundaries (arrows) assisted by cylindrical rollers, circular observation windows arranged around the channel, camera and mirror; (b) Side cut showing the channel, camera and optics, transmission, and underside pressure taps and gas distributors; (c) enlarged view of the channel.

The facility would have permitted gas-particle interactions to be studied over a range of conditions where suspensions are steady and fully-developed.

Unlike Earth-bound flows where the gas velocity must be set to values large enough to defeat the weight of particles, the duration and quality of microgravity on the Space Station would have generated suspensions where the agitation of the particles and the gas flow could be controlled independently by adjusting the gas pressure gradient along the flow, the relative motion of the boundaries, and the absolute pressure of the cell.

We planned two series of space flight tests. The first series, which we called "Viscous Dissipation Experiments," was meant to characterize the viscous dissipation of particle velocity fluctuation energy, when there is no relative mean velocity between gas and solids. To do so, we would have reduced the boundary speed in successive tests until the inertia of the solid particles became small enough for the particle motion to be affected by viscous forces in the gas. By evacuating the cell partially, we would have also investigated the role of the molecular mean free path in dissipating particle agitation. The Viscous Dissipation experiments would have tested theories predicting the detailed behavior of processes, like fluidized beds, which bring into contact gas and solid particles.

In a second series of tests, which we called "Viscous Drag Experiments," a gas pressure gradient would have been imposed on the shearing cell. The gradient would have induced a relative velocity between the two phases, while the shearing would have set the solids agitation independently. These Viscous Drag Experiments would have shed unique light on a important regime where particle velocity fluctuations are determined by a mechanism other than interactions with the gas. In this regime, we would have measured the dependence of the drag coefficient on the solid volume fraction and agitation of the solid particles. Partial evacuation would have also allowed us to test the effects of particle Reynolds number on the drag coefficient. The Viscous Drag experiments would have tested theories relevant to processes with significant relative velocity between gas and solids, such as pneumatic transport, catalytic cracking, circulating fluidization, and particle separation.

This project passed the Science Concept Review in May 2000. Our role was to refine the Science Requirements and to assist NASA-Glenn in developing flight hardware. Successive delays postponed work on the Requirement Design Review until cancellation of the project in 2005. To inform the design of the experiment, we conceived, manufactured and successfully tested a prototype of the apparatus on the KC-135 microgravity aircraft. Unfortunately, the aircraft could not provide the long-duration and high quality of microgravity required of the experiment, thus making it necessary to fly it on any of the available space platforms such as a sounding rocket, the Space Shuttle, or the ISS. In addition to our own KC-135 trials, NASA briefly devoted resources to create a smaller version of the SiGMA apparatus to be flown in the Microgravity Science Glovebox (MSG). Our proposal to do so was approved in early 2000, but cancelled in November 2001.

To interpret the experiments, we developed a theory predicting the development of the gas-solid flow in the channel. Our prototype demonstrated feasibility of the flight experiments, and suggested ideas for simplifying its operations and measurement techniques.

In summary, we conceived a fundamental gas-solid experiment with relevance to space exploration and industrial applications, derived an appropriate theoretical framework to predict its behavior, published the corresponding results, constructed a prototype, successfully tested the latter on the KC-135, wrote a complete set of science requirements, passed NASA's Science Concept Review, and trained and assisted the NASA-GRC team and contractors charged with its implementation as a flight experiment.

Despite its sudden cancellation, the SiGMA investigation led to the publication of scientific results, the education of undergraduate and graduate students, and the design of an experiment that remains worthwhile to fly on extended microgravity platforms. This report sums up our efforts and accomplishments in this project. Manuscripts and data published in the open literature are mentioned but not reproduced here for brevity.

2 Chronology

Following the award of our proposal in February 1998, and the project kick-off meeting at NASA-GRC in March, we wrote a Science Requirements Document (SRD) [1] and passed the corresponding Science Concept Review (SCR) in front of a panel of peer-scientists in June 2000. The science requirements were subsequently refined following the panel's recommendations and presented in an interim "Final" Technical Report [2] closing the first four-year funding period in March 2002. The project was renewed from January 2002 to December 2005 to allow us to finalize the science requirements and to assist NASA-GRC in its development of the flight experiment and procedure.

Conscious of the significance of our research to industrial processes, the International Fine Particle Research Institute, a consortium of the leading companies involved with powder processes, also

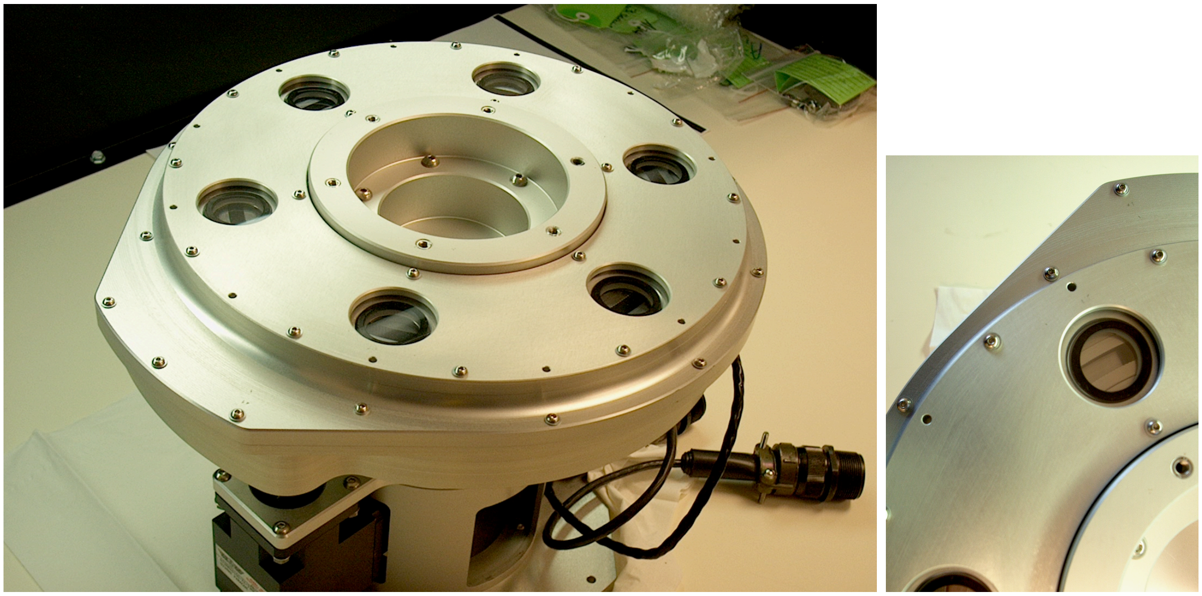

Figure 2: Photographs of μSiGMA flight hardware. Detail near one the windows showing the channel.

provided funding from October 1999 to November 2002 to assist in the development of a prototype apparatus.

In addition, following our proposal of July 1999, NASA decided in February 2000 to develop a smaller prototype apparatus for the MSG. The Science Design Review of this "μSigMA" project took place in June 2001 following the complete design and construction of flight hardware and appropriate controls by the NASA-GRC team led by Ronald Sicker (Fig. 2). Cut-backs forced the μSiGMA project cancellation in November 2001.

Meanwhile, we designed and built two prototypes of the eventual flight experiments. The first, which we shared with Professor Jenkins' "Micro-gravity Segregation of Energetic Grains" (μgSEG) flight project, was completed and successfully tested on the KC-135 in February 1998. It consisted of a "racetrack" shear cell with a moving inner bumpy boundary entraining two different kinds of spherical grains around the channel (Fig. 3). Its purpose was to examine the segregation of agitated grains that is driven by gradients of fluctuation energy perpendicular to the moving boundary. The straight section of the track was meant to establish a fully-developed flow that is independent of distance along the track and is not affected by centripetal accelerations.

Because the μgSEG project focused on the dynamics of granular flows with particle inertia much larger than gas-solid interaction forces, it could run with much higher speeds than the SiGMA experiment, for which solid inertia forces had to be of similar or smaller magnitude than drag forces from the surrounding gas. Consequently, unlike the SiGMA project, μgSEG did not require very long microgravity duration, and data acquired on the KC-135 with relatively large boundary speeds did yield meaningful results, albeit somewhat corrupted by g-jitter [3, 4, 5]. Such tests led by the PI took place at Lewis Field of NASA-GRC in February 1998, June 1998, September 1998, June 1999, September 1999, and March 2000. The Cornell μgSEG cell prototype was used in all campaigns except September 1999 when we tested a version designed by the NASA-GRC team led by Joseph Balombin.

One of the lessons of the racetrack prototype was that granular flows could not develop fully in a straight section. Our numerical simulations and theory revealed that the curved sections of the track had a pervasive influence on the flow [6, 7]. Accordingly, we designed the second prototype for SiGMA with an axisymmetric channel featuring two independent moving boundaries, see Fig. 4. In this case, we showed that centripetal accelerations are negligible as long as the distance between the circular moving boundaries is small compared with their radius [2, 8].

The SiGMA project included two principal test series. The first, which we dubbed "Viscous Dissipation Experiments," was meant to record the damping of granular agitation by the surrounding air. To do so, it would suffice to shear a single kind of spheres between the inner and outer boundary of the channel at progressively smaller speeds. Inertial forces of the grains would decrease with decreasing speed, and thus begin to be dominated by viscous forces imparted by the surrounding air on the grains. This experiment is impossible to run on Earth, where gravity would promptly force the slow spheres to the bottom of the channel. Instead, long-duration microgravity would maintain the grains in suspension with fluctuation velocities scaling with boundary cell speed. Any departure from that scaling would have revealed the role played by viscous forces of the gas. It is important to understand this role, as it governs the behavior of any gas-solid suspension, such as a fluidized bed of Geldart group A- or C-powder, in which the relative velocity between gas and solids is small.

In another series of experiments, which we called "Viscous Drag Experiments," we planned to investigate cases where the relative velocity is not small. In traditional models, the role of such relative velocity is captured by an overall drag coefficient that yields the force between the gas and solid phases. However, no experiment has yet revealed whether or how this coefficient is affected by particle agitation. Generally, the coefficient is fit from tests where the solid phase is fixed. More complex experiments, such as fluidized beds, bring into contact agitated particles and a cross-flow of gas. However, because on Earth the gas keeps particles suspended through its mean relative velocity with the solids, and because in doing so it imparts velocity fluctuations to the solids, fluidized bed experiments have hitherto made it impossible to decouple the role played by the relative gas-solid velocity and that of the solid agitation.

Accordingly, we designed the SiGMA experiment to provide solid agitation independently from gas drag. This experiment crucially depended upon accurate measurement of air flowing through all sections of the channel. While it was straightforward to record the overall gas flow rate injected in the cell, it was less so to find out how much gas would choose to flow along the granular flow in the "co-flow" section of the channel, and against it in the "counter-flow" section (Fig. 5).

At the SCR, we had envisioned to measure the gas flow rate by injecting small fluorescent particle tracers along with the air flow, to record local gas velocities from the corresponding tracer streaks visible in each image, and to integrate the resulting gas velocity profile in the width of the cell. In this way, we would have exploited the same high-speed camera system to visualize grain and gas velocities simultaneously. Despite having conducted successful test of this technique in a small laboratory setup at Cornell, it became rapidly evident to us that the development of this system for the entire SiGMA shear cell would be difficult. In particular, we could not easily prevent contamination of the entire cell with a myriad shiny small tracer particles adhering onto grains,

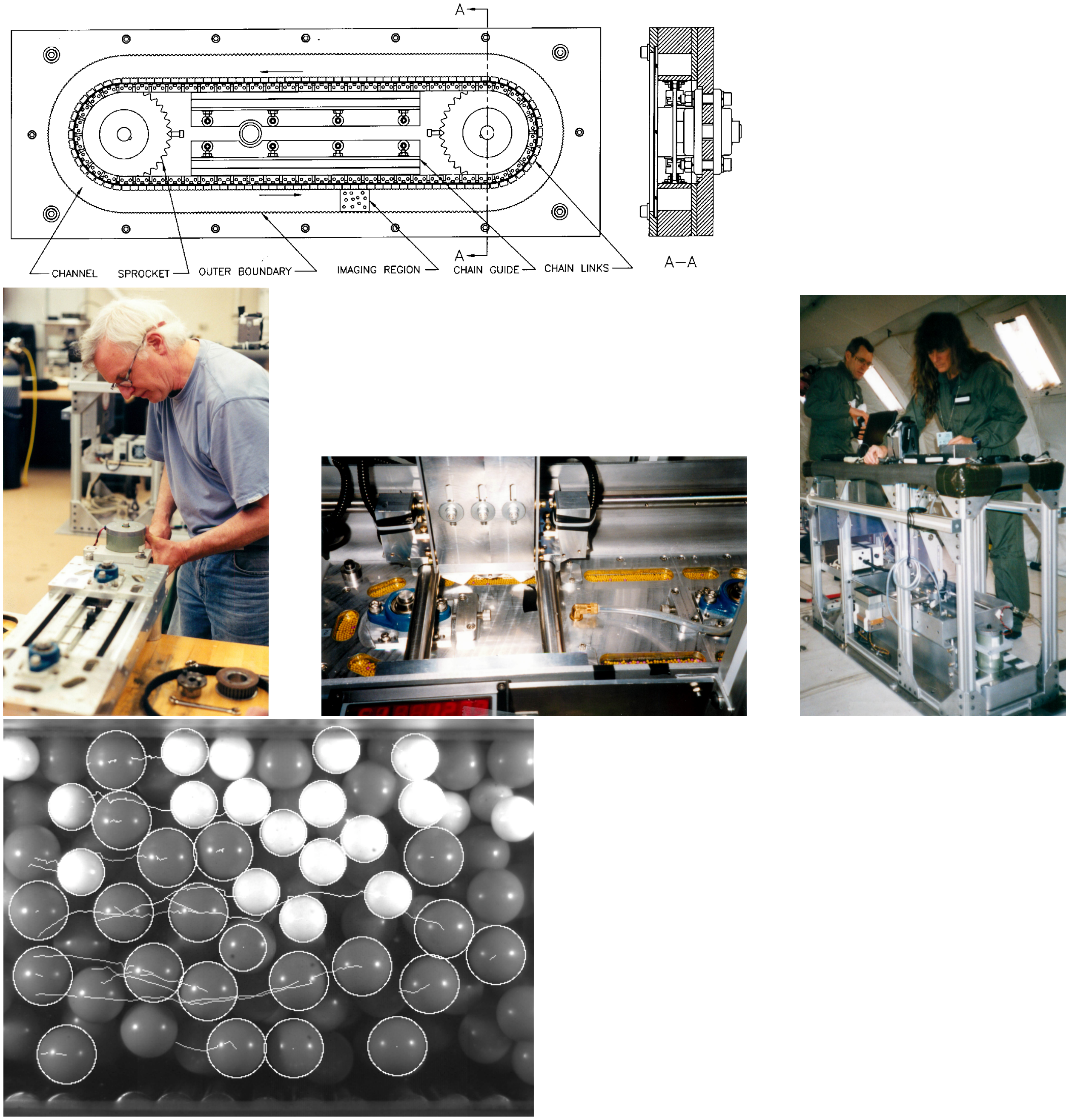

Figure 3: Photographs of μgSEG racetrack. From left to right and top to bottom: top view; Stephen Keast assembling the apparatus for tests; close-up with a mixture of yellow 3mm and purple 4 mm acrylic spheres; apparatus mounted on the KC-135 rig; high-speed camera image of a binary mixture of white 3mm ceramic and 4 mm purple acrylic spheres with superimposed computer vision tracking of the sphere centers over several images; the moving boundary appears at the bottom of this picture.

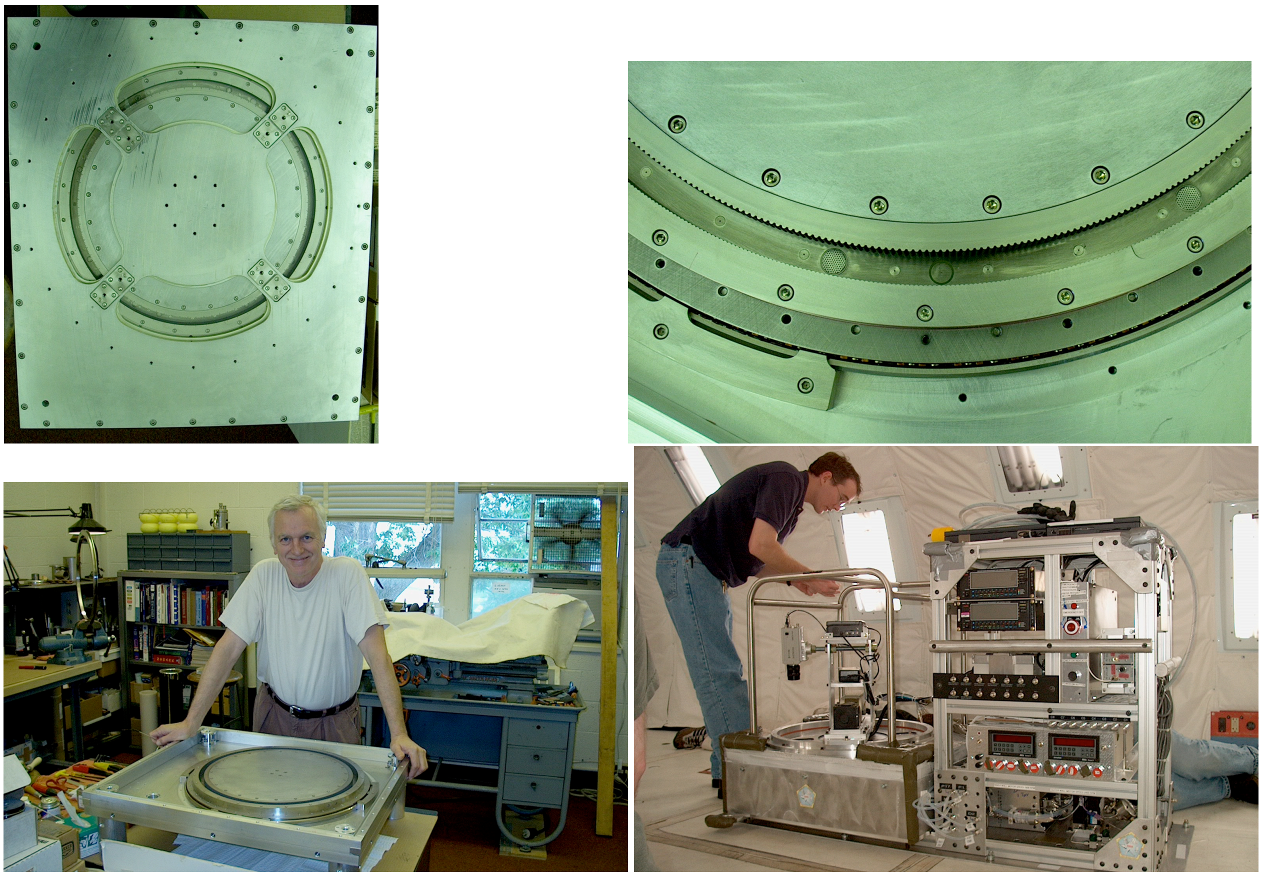

Figure 4: Photograph of the axisymmetric SiGMA prototype. From left to right and top to bottom: top view showing the circular channel beneath four large glass windows; detail of the channel featuring at its base, from left to right, three static pressure taps, a gas distributor with a mesh filter, another pressure tap, the sensor of a capacitance probe, three pressure taps, another distributor, and another tap. Stephen Keast and his creation. The cell incorporated on the KC-135 rig, including its motor controls for inner and outer boundaries, static pressure measurement and control system, capacitance probe system, gas manifold, high-speed camera system, and computer data acquisition and control.

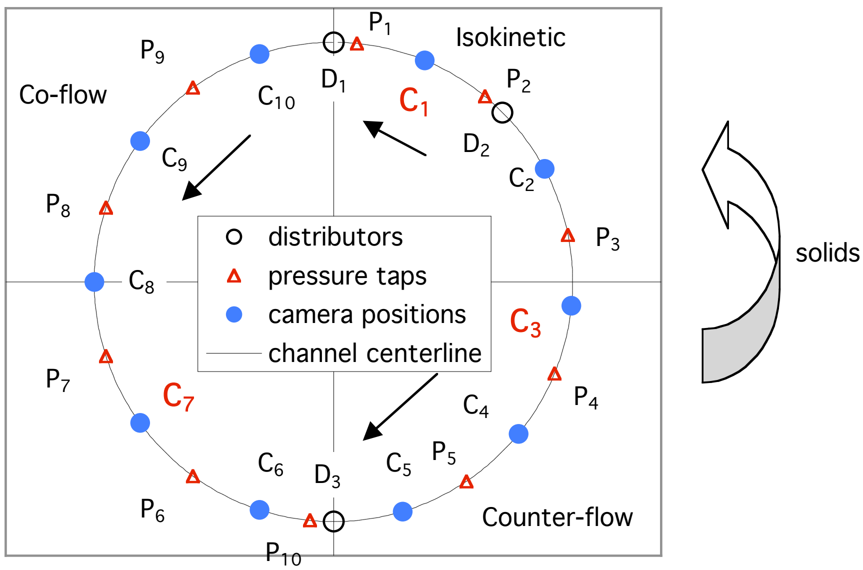

Figure 5: Sketch of gas distribution along the SiGMA shear cell. The large arrow to the right indicates the general direction of the granular flow, while the smaller black arrows point that of the gas flow. Static pressure taps located at P_i with $i = 1, 10$ are drilled through the base of the narrow channel. Most of the air is introduced through the base with a distributor located at D_1. It can split two ways: to the left along the "co-flow" section; and two the right along the "counter-flow" section. To determine the relative proportion of these two gas streams, enough additional air is injected at distributor D_2 to cancel the static pressure drop between P_1 and P_2 across the "isokinetic" section. There, because the mean drag between gas and solids vanishes, the gas flow rate can be simply inferred from video measurements of mean granular velocity and average solid volume fraction. To record the latter along the channel, capacitance sensors are located at positions C_i with $i = 1, 10$. All gas is withdrawn at distributor D_3.

walls, and windows.

While the GRC design team led by John Caruso persisted in developing a tracer method, we devised a simpler alternative sketched in Fig. 5. Its principle was to operate a control systems that injects enough air into a third distributor to cancel the pressure drop across a small "isokinetic" section of the cell. Such pressure drop can only vanish if there is no relative velocity between grains and gas. In this case, we could use the high-speed camera system to record the transverse profiles of mean granular velocity in the isokinetic section, and infer the corresponding mean velocity of the gas, and then its volume flow rate, using independent measurements of the mean solid volume fraction from capacitance probes.[1] [2]

We verified the feasibility of the control system and the capacitance probes in the axisymmetric prototype in two campaigns of the KC-135 in March and April 2002. Although the airplane could not produce microgravity long enough for actual SiGMA experiments, we produced again useful data for the μgSEG project and we demonstrated our simpler strategy for recording gas volume flow rates [2].

We spent the remainder of the NASA contract on the following tasks: (1) finalizing the science requirements shown in the Appendix; (2) producing an exhaustive "interactive" test matrix that allowed designers of the apparatus to check any trade-offs against these science requirements and associated minimum success criteria; (3) answering questions and training the NASA-GRC design team and its contractors ZIN Technologies and MK Optics & Vision in their design and testing of optical and mechanical breadboards; (4) refining the theory and numerical codes to predict the behavior of the cell using available correlations for drag and constitutive relations; (5) supporting the design with various calculations, as summarized below; (6) selecting spherical grains of a material minimizing electrostatic charging, parasitic magnetic forces, and energy dissipated in impacts with walls, windows and other spheres; (7) carrying out additional research on granular flows and heat transfer in other configurations of interest to ISRU and industrial applications; and (8) publishing the corresponding results.

3 Accomplishments

Although NASA could not muster resources needed to complete this project, scientific benefits have derived from it. We summarize these in three sub-section below: (3.1) publications; (3.2) student training and outreach; (3.3) supporting calculations and experiments communicated to NASA or relevant to other ISRU contexts.

Briefly put, our principal science results are (1) the first quantitative reconciliation of KC-135 microgravity experiments, molecular dynamic simulations and theory for collisional granular flows and their segregation in a wall-bounded channel; (2) the creation of algorithms for solving the governing equations of the theory; (3) the development of computer vision techniques for measuring granular

[1] M. Louge, M. Tuccio, E. Lander and P. Connors: "Capacitance Measurements of the Volume Fraction and Velocity of Dielectric Solids Near a Grounded Wall," *Rev. Sci. Instrum.* **67** (5), 1899-77 (1996).

[2] M.Y. Louge: US patents 5,546,006 and 5,459,406 "Guarded capacitance probes for measuring particle concentration and flow," (1995 & 1996).

temperature and the derivation of a formal theory for predicting the corresponding uncertainties; (4) the design of long-term microgravity experiments to test the theories of Sangani, et al,[3] and others, for the interactions between a gas and agitated grains (SiGMA); (5) the design of similar experiments to test the theories of Jenkins and Mancini,[4] and others, for the segregation of binary mixtures of inelastic spheres (μgSEG); (6) the development of a new theory for granular flows down a rough inclined base and down a flat, frictional plane [9]; the corresponding elucidation of the data of Pouliquen[5] and Silbert et al.[6] for a rough base and of our own experiments on a flat, frictional plane; (7) the development of a new theory for the enhancement of wall heat transfer by agitated solids suspended in a gas [10]. The last two items are relevant to ISRU and industrial applications.

3.1 Publications

Publications resulting from data and models developed in the SiGMA project are marked with an asterisk* in the references below. Other publications of fundamental science relevant to ISRU and acknowledging NASA support are also listed there.

Details of the experiments, its principles, measurement techniques, prototype tests, theory and ancillary calculations appear in the SRD [1], interim final report [2], and Haitao Xu's PhD thesis [7]. Other documents, such as the final science requirements reproduced in the Appendix, the definition of "success criteria", and the "interactive" test matrix helping designers of the flight experiment juggle various trade-offs, were communicated and explained to NASA-GRC personnel during the SiGMA project.

We also summarized salient ideas and results in the open literature, albeit with less detail. Topics included the flow development of sheared granular flows along the racetrack cell used in μgSEG [6], the principle of our Viscous Dissipation [8] and other gas-solid experiments [11], comparisons with numerical simulations of our theoretical predictions for the behavior of sheared agitated granular mixtures undergoing segregation [4] or suspended in a viscous gas at low to moderate Reynolds numbers [11, 12], rigorous calculations of uncertainties in granular agitation (or "temperature") measured from grain positions in consecutive high-speed images [5], selected results revealing anomalies for the impact of spheres on flat walls [13], and other granular mechanics results relevant to ISRU [14]-[22].

3.2 Education and Outreach

The SiGMA project was conducted by the Cornell PI (M. Louge) and co-I (J. Jenkins), by a professor with expertise in computer vision (A. Reeves), by a technician (S. Keast), and by two graduate students (H. Xu and X. Chen) who obtained their PhD with NASA funding.

[3] Sangani A.S., Mo G., Tsao H.-K., and Koch D.L., "Simple shear flows of dense gas-solid suspensions at finite Stokes number," *J. Fluid Mech.* **313**, 309-341 (1996).

[4] Jenkins, J.T., Mancini, F., " Kinetic theory for binary mixtures of smooth, nearly elastic spheres," *Phys. Fluids A* **1**, 2050-2057 (1989).

[5] Pouliquen O., "Scaling laws in granular flows down rough inclined planes," *Phys. Fluids* **11**, 542-548 (1999).

[6] Silbert L., Ertas D., Grest G., Halsey T., Levine D., and Plimpton S., "Granular flow down an inclined plane: Bagnold scaling and rheology," *Phys. Rev. E* **64**, 051302 (2001).

SiGMA also supported 44 undergraduate and Master of Engineering projects at Cornell. Their role was to record impact parameters for spherical particles used in the experiments and to assist the development and construction of the prototype cells. This team won the 2001 Cornell Society of Engineers award for leadership in undergraduate research.

Students included Edward Balaban, Taro Banno, Chris Salvestrini, Sam Vonderheide, Greg Aloe†, Josh Freeh, Lance Hazer, Rowin Andruscavage, Patrick Florit, Claudio Bazzichelli, Rami Sabanegh, Steven Gutierrez, Amelia Dudley†, Michael Garon, Priscilla Carreon, Peter Weisz†, Brooks Haxton, Michael Adams†, Jenny Moose, Musyoka Munyoki†, James Buckley, Reno Giordano, James Chun, Farshid Azad, Sean McCann OBrien, Siddharth Sinha, Sharon Ang, Attakrit Asvanunt, Donald Casey, Andrew Seow, Sewan Kim, Kiril Savov, Yuenan Wang, Joonil Kwak, Matthew Crozier, Andrew Lapsa, Ed Palermo, Dave Tagatac, Victoria Law, Renee Hillaire, Christopher Fontana, Emmanuel Franjul, Matthew Robb, and Cheryl Sorace.[7]

Professor Louge also ran a program in which undergraduates teach Technology Education to eighth graders at Ithaca's DeWitt Middle School. Thirty Cornell students have done so since 2000. He also advised the Odysseus undergraduate team, which competed in NASA projects related to Space Exploration. The team was the "Technical Runner-up" in 2001, and a finalist in 2002, 2003 and 2004.

In another outreach program, Professor Louge led the US delegation to the Second International Conference on the Formation and Migration of Dunes in Nouakchott, Mauritania (2001). The delegation, which was sponsored by NASA, discussed Martian and terrestrial dunes, and held conversations with cabinet ministers on education and dune remediation techniques. He also chaired the Second Gordon Conference on Granular and Granular-Fluid Flow in Colby College, Maine, June 27 to July 2, 2004.

The PI delivered talks publicizing the SiGMA and μgSEG projects, as well as other research sponsored by NASA. We provide here a selection of invited seminars, excluding contributed talks:

[1] "Granular segregation and gas-particle interactions in a microgravity flow cell," Illinois Institute of Technology, Chemical Engineering Department, November 29, 2000.

[2] "Granular segregation and gas-particle interactions in a microgravity flow cell," Stevens Institute of Technology, Mechanical Engineering Department, December 6, 2000.

[3] "Granular and gas-solid flow research at Cornell," Caltech, College of Engineering, February 27, 2001.

[4] "Granular Flow Module," invited talk to the Committee on Microgravity Research, Space Studies Board, National Research Council, April 18, 2001.

[5] "Microgravity on a plane!" Kopernik Center, Vestal, NY, August 8, 2001.

[6] "Granular flows with collisional and enduring contacts," invited seminar, University of Kyoto, Japan, July 18, 2002.

[7] "On dense granular flows down bumpy inclines," invited seminar, Mechanical Engineering

[7] Students marked with † took part in the microgravity tests on the KC-135.

Department, New Jersey Institute of Technology, September 18, 2002.

[8] "Models of impact," invited seminar, Department of Mathematics, New Jersey Institute of Technology, September 20, 2002.

[9] "Etudes de Milieux Granulaires Agités," Université de Rennes I, GMCM, invited seminar, June 27, 2003.

[10] "On Dense Granular Flows down Bumpy Inclines," invited talk, Purdue University, February 5, 2004.

[11] "Can dense granular flows down inclines be modeled using kinetic theory?," invited talk, Department of Applied Mathematics & Theoretical Physics, University of Cambridge, November 21, 2005.

[12] "Les Physiciens ont un Grain," Année Mondiale de la Physique 2005, invited talk at the "Institut de Physique de Rennes," December 9, 2005.

[13] "Density invariance and fluctuation energy for granular flows on rigid, bumpy inclines," invited seminar, ESPCI, Paris, April 7, 2006.

[14] "Thermal transport in suspensions of gases and agitated solids," invited seminar, Ecole Polytechnique de l'Université de Nantes, April 13, 2006.

[15] "Ecoulements gravitaires sans parois latérales sur fond rugueux," Université de Rennes 1, July 10, 2006, invited seminar.

[16] "Granular flows, and surface density on desert dunes," invited seminar, University of Chicago, Franck Institute, October 9, 2006.

[17] Gordon Research Conference on Granular & Granular-Fluid Flow, Oxford, July 23-27, 2006. Discussion leader, session on chute flow. "Granular Flows down Inclines, Discussion," invited review, July 24, 2006.

[18] "Density invariance and fluctuation energy for granular flows on rigid, bumpy inclines," Eid. Schnee u-Lawinen Forschung, invited talk, Davos, March 15, 2006.

[19] "The significance of granular flows to Lunar and Martian exploration," Gordon Research Conference on Engineering Sciences for Space Exploration, August 22, 2005, Les Diablerets, Switzerland, invited keynote talk.

[20] Kavli Institute for Theoretical Physics, UC Santa Barbara: invited talk on June 20, 2005. "Granular flows down inclines with and without side walls."

[21] Workshop on Granular Materials in Lunar and Martian Exploration: Kennedy Space Center, "Granular Flow Challenges in Lunar and Martian Exploration," February 2, 2005, invited talk.

[22] "Collisional Granular Flows with and without Gas Interactions in Microgravity," Mini-Symposium Invited lecture at ICTAM 2004, in the mini-symposium on "Microgravity Flow Phenomena," 21st International Congress of Theoretical and Applied Mechanics, Warsaw, Poland August 16, 2004.

[23] GDR Midi, Carry-le-Rouet, France, "Le rôle du moment angulaire dans les écoulements

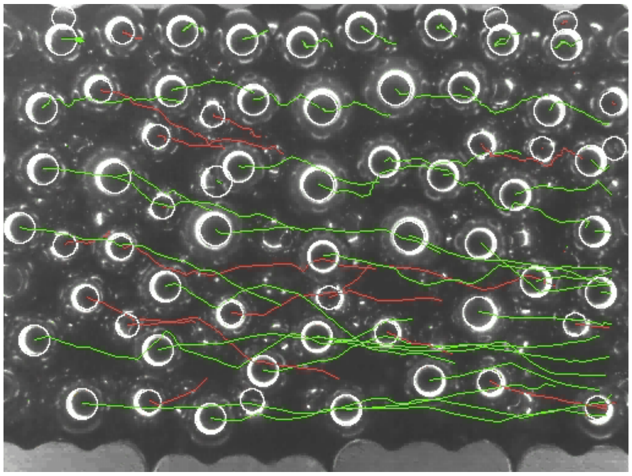

Figure 6: A typical picture of a binary mixture of shiny spheres and the corresponding trajectories computed by the vision software from successive position of ring light reflections in the racetrack prototype operated on the KC-135.

gravitaires," invited talk, June 8, 2004.

[24] "Role of Couple Stresses in Shallow Granular Flows down a Bumpy Incline," 5th International Conference on Multiphase Flow, ICMF'04, Yokohama, Japan, keynote speech, June 2, 2004.

[25] "Granular Segregation in Collisional Shearing Flows," invited talk, Newton Institute, Cambridge, UK, September 23, 2003.

[26] "Interactions between a gas and dispersed solids at moderate Stokes numbers," keynote speech, Engineering Foundation Conference on Fluid-Particle Interactions VI, Barga, Italy August 29, 2002.

[27] "Granular flows in open and closed channels," invited lecture, Gordon Research Conference on Granular and Granular-Fluid Flow, Plymouth, NH, July 4, 2002.

[28] "Boundary conditions, friction and particle interactions," invited presentation, Disperse Flow Study Group, Workshop on Scientific Issues in Multiphase Flows, U. of Illinois at Urbana-Champaign, May 7, 2002.

[29] "NASA's Granular Flow Module," AUI/ISSI NorthEastern Regional Meeting, November 1, 2001.

[30] "Microgravity segregation in collisional granular shearing flows," keynote talk, Mechanics for a New Millennium, ICTAM-2000, Chicago, August 29, 2000.

[31] "A Review of Selected Measurement Techniques for Dense Gas-Solid Suspensions," Winter Annual Meeting of the AIChE, Dallas, November 3, 1999.

[32] "Advances in Experimental Methods," keynote talk, Engineering Foundation Conference on Fluid-Particle Interactions V, Santa Fe, NM, May 12, 1999.

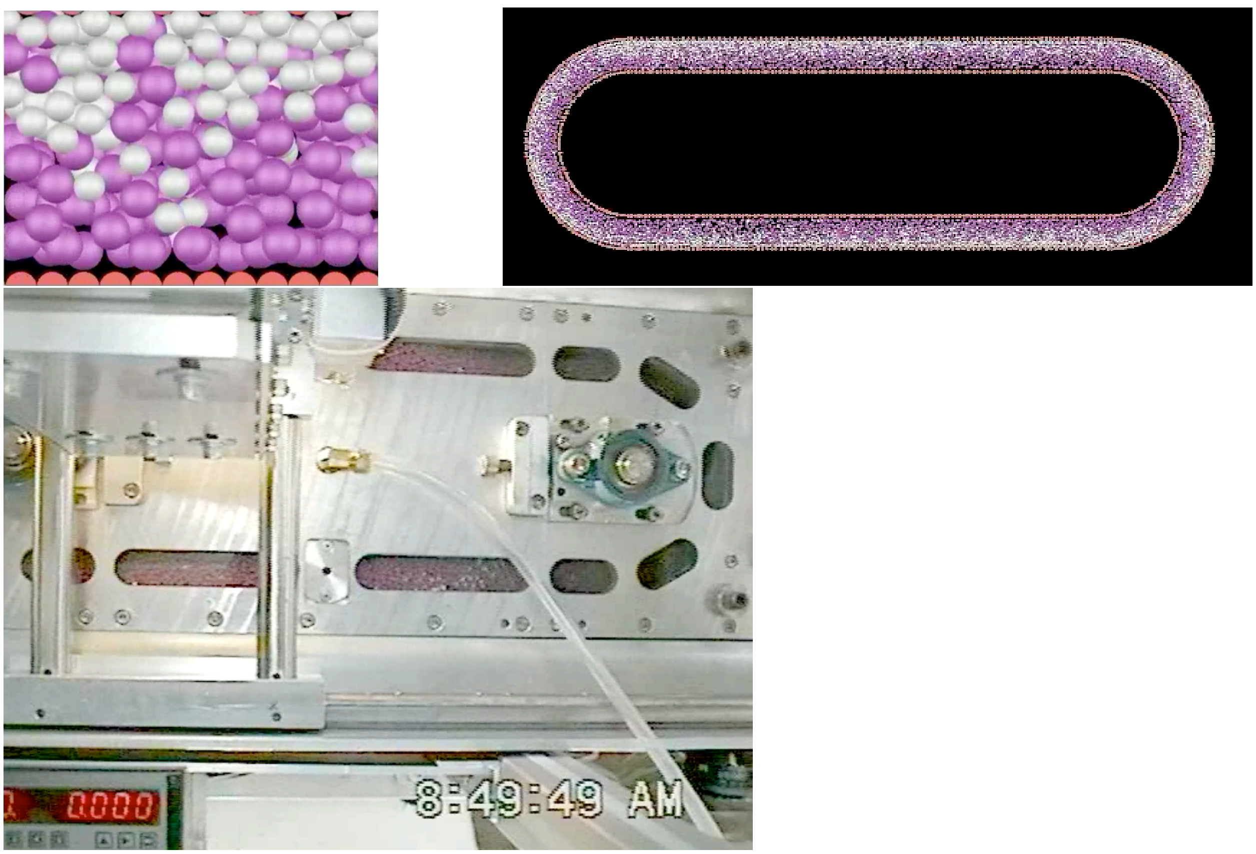

Figure 7: Output of the simulations of the racetrack shear cell. Left: detail near the observation window. Right: view of the entire cell. Bottom: the corresponding experiment on the KC-135.

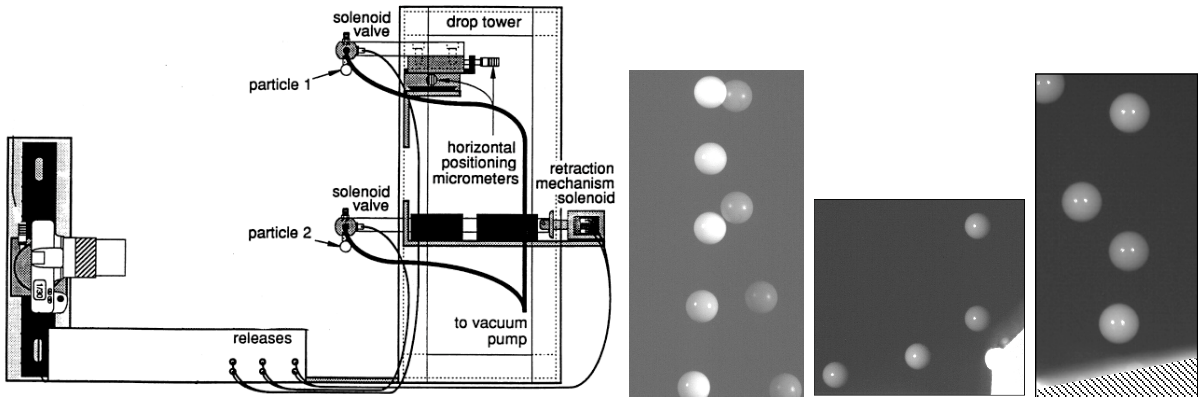

Figure 8: From left to right: Sketch of the binary impact facility. Stroboscopic pictures of a binary collision of a ceramic and an acrylic sphere; of an acrylic sphere on a single bump; of a ceramic sphere on a flat window.

3.3 Supporting calculations

We supported NASA's engineering team by predicting the performance of the SiGMA and μgSEG shear cell, and by providing calculations on crucial design items. These included:

[1] The development of fully-functional software and graphical user interfaces for the tracking of spheres from digital video images. The calculation of the resulting profiles of mean and fluctuation velocities [4, 5] (Figs. 3, 6).

[2] The development of a ring-light system to visualize reflective spheres. Calculations of the ring produced on each sphere and incorporation of the corresponding model in the computer vision software (Fig. 6).

[3] The creation of software permitting the simulation of actual flows in the entire "racetrack" and axisymmetric microgravity shear cells, with realistic description of all boundaries and interparticle interactions (Fig. 7). The writing of a suite of subroutines to extract volume fraction oscillations, as well as all moments of angular and linear momenta up to the second order.

[4] The operation by undergraduate students of a unique facility to measure impact parameters among spheres, and between spheres and all types of walls used in the SiGMA and μgSEG experiments (Fig. 8).

[5] The development and successful tests of specialized capacitance instruments capable of recording the time-dependent solid volume fraction in the SiGMA cell, in the presence of conductive or dielectric spheres. The first implementation of such quantitative capacitance system with observation windows that are ITO-coated to act as reference voltage for the probes (Fig. 9).

[6] The development of a unique "isokinetic" system to record simultaneously the profiles of solid velocities up to the second moment of their fluctuations and the mean gas flow in the cell channel [7]. The demonstration of the system with Enrique Ramé's help at NASA-GRC in August 2002 and on the KC-135.

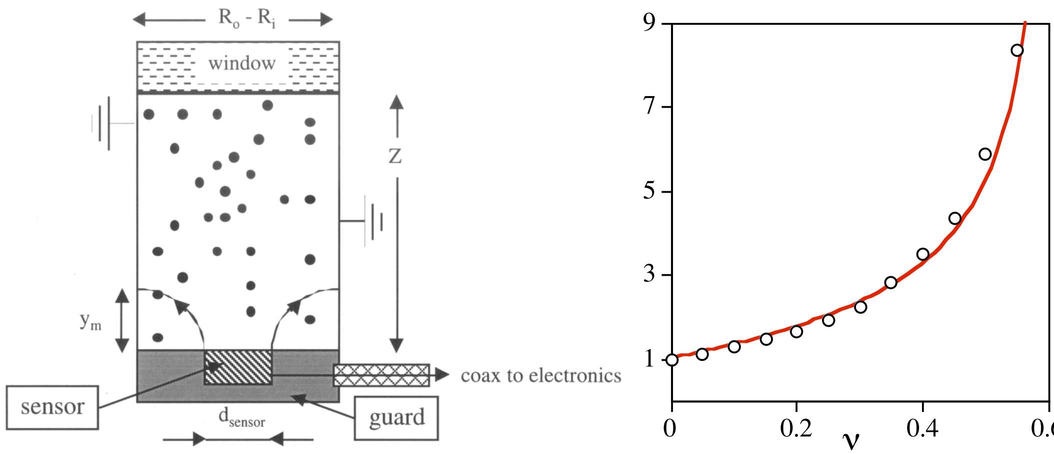

Figure 9: Left: sketch of the capacitance instrument in a cross-section of the SiGMA channel. Right: comparison between model (line) and test data (symbols) for the effective dielectric constant of shaken steel spheres.

[7] Calculations of the gas flow rate bypassing the main SiGMA cell channel through the clearance between stator and rotor. Derivation of the corresponding requirements and demonstration of the relative unimportance of this effect in the SiGMA prototype shear cell [2].

[8] ANSYS numerical simulations of deflections of the top and bottom SiGMA shear cell plates and windows under partial evacuation (Fig. 10), carried out by a Cornell MEng student.

[9] The development of an alternative optical technique to record the solid volume fraction profile from high-speed camera pictures using a limited depth of focus. Interpretation of the data using a new theory based on the HAB pair-distribution framework for spatial oscillations of the center-average solid volume fraction near a flat wall (Fig. 11). This method was proposed to the leadership of the engineering team as an alternative solid volume fraction measurement that would supercede the capacitance instrumentation, with which NASA lacked experience.

[10] The design and operation of a simple free-floating microgravity apparatus to evaluate qualitatively the propensity of various spheres to acquire static electrical charges (Fig. 12).

4 Acknowledgments

We are grateful to NASA for its funding and to the NASA personnel that made progress on the SiGMA project possible. It was a pleasure to work with NASA-GRC.

The SiGMA Project Scientist was Enrique Ramé, and the Project Managers were Joseph Balombin until January 2001 and then John Caruso. Ronald Sicker led the μSiGMA effort. They were assisted by engineers, managers and experts who included F. Gati, R. Butcher, C. Gallo, G. Haddad, T. Jacobson, J. Juergens, J. Kolis, R. Kortis, D. Kozlowski, R. Sicker, J. Larko, R. Manella, P. Mellor, B. Motil, E. Nelson, B. Ovryn, L. Rasberry, R. Snyder, K. Sukel, J. Withrow, G. Wroten, J. Yaniec, D. Noren, R. Helmick, M. Babula, R. Hakimzadeh, J. Mackey, R. Werner, F. Kmiecik,

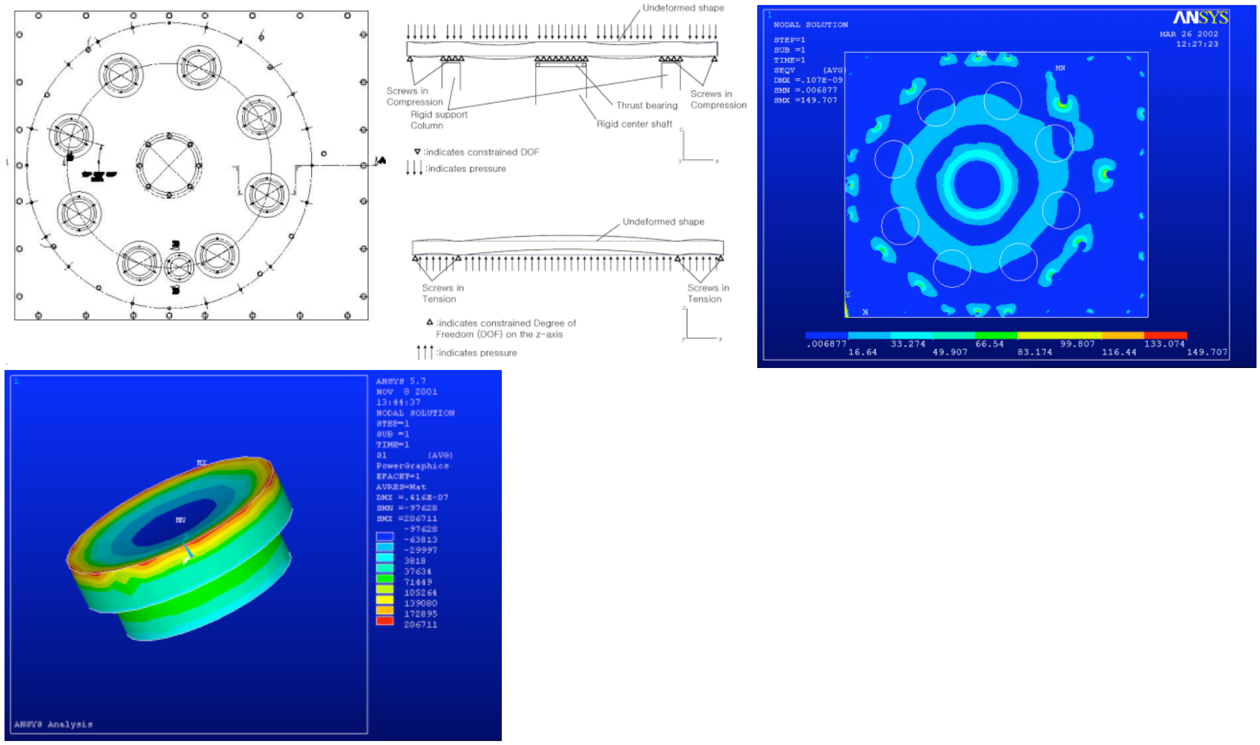

Figure 10: Left: ANSYS model of the top plate of the SiGMA shear cell; right: corresponding deflections. Bottom: Three-dimensional modeling of stresses in glass windows.

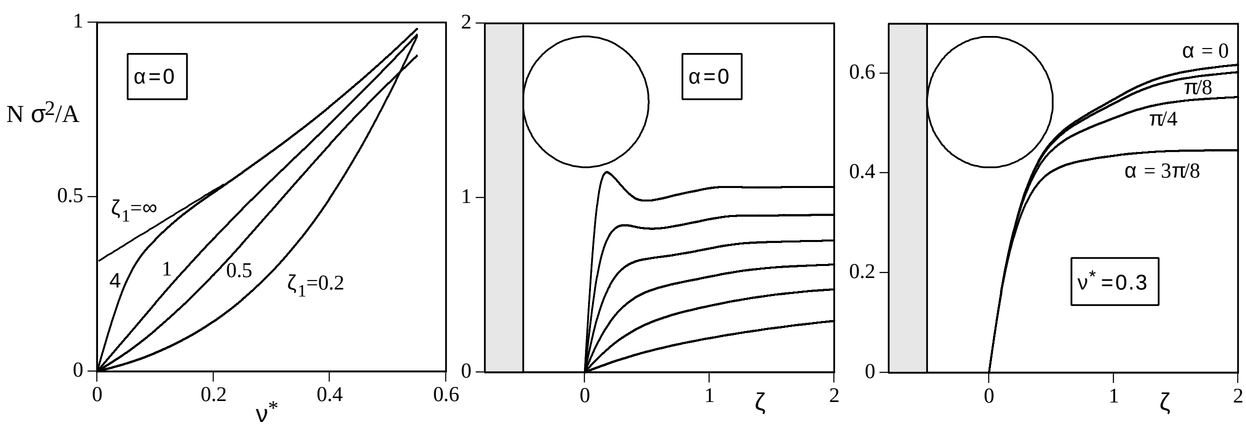

Figure 11: Number of detectable spheres with centers located within the window distance y such that $\zeta = \left(\frac{y}{\sigma} - \frac{1}{2}\right) \in \left[0, \zeta_1\right]$, made relative to the sphere diameter and the area of the window, versus bulk solid volume fraction ν^* for the values of ζ_1 shown and camera view angle $\alpha = 0$ (left); versus ζ_1 for $\alpha = 0$ and, from bottom to top, $\nu^* = 0.1$, 0.2, 0.3, 0.4, 0.5 and 0.6 (center); versus ζ_1 at $\nu^* = 0.3$ for the values of α shown (right).

Figure 12: Left: Michael Adams, a Cornell Mechanical Engineering undergraduate, releases the free-float experiment on the KC-135 during a period of microgravity. Right: A typical view from the video camera showing agitated steel spheres (left) and a denser collection of ceramic spheres (right).

W. Turner, N. Shaw, C. Lant, A. Wilkinson, B. Singh, F. Kohl, G. Pitalo, K. Kusanke, G. Fedor, K. McGinnis, C. Blaser, and E. Anderson.

References

[1] M. Y. Louge and J. T. Jenkins. Science Requirements Document for Studies of Gas-Particle Interactions in a Microgravity Flow Cell, May 2000.*

[2] M. Y. Louge and J. T. Jenkins. Final Technical Report for Studies of Gas-Particle Interactions in a Microgravity Flow Cell, NASA Contract NAG3-2112, March 2002.*

[3] M. Louge, J. Jenkins, H. Xu and B. Arnarson. Granular segregation in collisional shearing flows, in *Mechanics for a New Millennium*, A. Aref and J.W. Phillips, eds., Kluver Academic Publishers (2001), pp. 239-252.*

[4] H. Xu, M. Louge and A. Reeves. Solutions of the Kinetic Theory for Bounded Collisional Granular Flows. *Continuum Mechanics and Thermodynamics*, 15: 321-349 (2003).*

[5] H. Xu, A. P. Reeves and M. Y. Louge. Measurement Errors in the Mean and Fluctuation Velocities of Spherical Grains from a Computer Analysis of Digital Images. *Rev. Sci. Instrum.* **75**, 811-819 (2004).*

[6] H. Xu, M. Louge and J. T. Jenkins. Flow development of a sheared collisional granular flow, in *Powders and Grains 2001*, Y. Kishino, ed., Swets & Zeitlinger, Lisse, pp. 359-362 (2001).*

[7] Haitao Xu. Collisional granular flows with and without gas interactions in microgravity. *Doctoral thesis*, Cornell University (2003).*

[8] M. Louge, H. Xu and J. T. Jenkins. Studies of Gas-particle Interactions in a Microgravity Flow Cell, in *Powders and Grains 2001*, Y. Kishino, ed., Swets & Zeitlinger, Lisse, pp. 557-560 (2001).*

[9] M. Louge and S. Keast. On Dense Granular Flows Down Flat Frictional Inclines. *Phys. Fluids* **13**, 1213-1233 (2001).

[10] Xinglong Chen. Thermal transport in suspensions of gases and agitated solids. *Doctoral thesis*, Cornell University (2006).

[11] M. Louge and H. Xu. Collisional Granular Flows with and without Gas Interactions in Microgravity, in *Mechanics of the 21st Century*, W. Gutkowski and T.A. Kowalewski, eds., Springer, Dortrecht, The Netherlands (2005), pp. 229-240.*

[12] H. Xu, R. Verberg, D. Koch and M. Y. Louge. Dense bounded shear flows of agitated solid spheres in a gas at intermediate Stokes and finite Reynolds numbers. *J. Fluid Mech.*, submitted (2007).*

[13] M. Y. Louge and M. E. Adams. Anomalous behavior of normal kinematic restitution in the oblique impacts of a hard sphere on an elasto-plastic plate. *Phys. Rev. E* **65**, 021303 (2002).*

[14] R. Delannay, M. Louge, P. Richard, N. Taberlet, and A. Valance. Towards a theoretical picture of dense granular flows down inclines. *Nature Materials* **6**, 99-108 (2007).

[15] M. Louge, A. Valance, N. Taberlet, P. Richard and R. Delannay. Volume fraction profile in channeled granular flows down an erodible incline, in *Powders and Grains 2005*, H.Herrmann, G. Gudehus, S. Luding, & K. Sommer (eds), A. Balkema, NY, pp. 885-889 (2005).

[16] N. Taberlet, P. Richard, R. Delannay and M. Louge,. How sidewalls influence granular flows, in *Powders and Grains 2005*, H.Herrmann, G. Gudehus, S. Luding, & K. Sommer (eds), A. Balkema, NY, pp. 873-876 (2005).

[17] M. Louge. Scientific issues in the flow of gases with dispersed solids. *Multiphase Science and Technology* **15**, 1-5 (2003).*

[18] M. Louge. Model for dense granular flows down bumpy inclines. *Phys. Rev. E* **67**, 061303 (2003).

[19] M. Y. Louge, J. T. Jenkins, A. Reeves and S. Keast. Microgravity segregation in collisional granular shearing flows, in *Proceedings of the IUTAM Symposium on Segregation in Granular Materials*, A. D. Rosato and D. L. Blackmore, eds., Kluver Academic Publishers, Boston (2000), pp. 103-112.*

[20] B. Ö. Arnarson, J. T. Jenkins and M. Y. Louge. Particle Segregation in Collisional Shearing Flows, in *Proceedings of the IUTAM Symposium on Segregation in Granular Materials*, A. D. Rosato and D. L. Blackmore, eds., Kluver Academic Publishers, Boston (2000), pp. 223-229.*

[21] J. Jenkins and M. Louge. Microgravity segregation in binary mixtures of inelastic spheres, in *Powders and Grains 97*, R. Behringer and J. Jenkins, eds, A.A. Balkema, Rotterdam (1997), pp. 539-542.*

[22] R. A. Wilkinson, R. P. Behringer, J. T. Jenkins and M. Y. Louge. Granular materials and the risks they pose for success on the Moon and Mars, in *Space Technology and Applications International Forum 2005*, American Institute of Physics (2005).*

Appendix EXPERIMENTAL REQUIREMENTS

5.1. Science Requirement Summary Table -- Revised 5/20/04

Parameter	Section	Requirements
Shear cell	5.2.1	Axisymmetric, rectangular test section, independently moving bumpy boundaries, flat metal base, clear windows, $Y'/\bar{R} \le 1/15$. Viscous Drag: controlled gas injection and withdrawal, pressure taps.
Dimensions	5.2.2	$R_i/d = 104.1 \pm 1\%$; $R_o/d = 113.2 \pm 1\%$; $Z/d = 10 \pm 1\%$; $(Ro\text{-}R_i)/d = 9.1 \pm 2\%$; $d_i/d = 1.0\ (\pm 1\%)$; $d_o/d = 1.0\ (\pm 1\%)$. $\Delta_i\ /d=0.5\ (\pm 1\%)$, $\Delta_o\ /d=0\ (+ 1\%)$. Record design dimensions to within 25μm. Provide a sample with a single bump to Cornell for impact testing and approval.
Conditions	5.2.3	$\bar{\bar{v}}$, p_g, ω_o, ω_i, Q see test matrix workbook "SiGMA_mgSEG_testmat_5-20-04.xls". Viscous dissipation: worksheet "VisDiss"; Viscous Drag: worksheet "VisDrag(3dist)".
Moving boundaries	5.2.4	Set ω_i and ω_o as shown in the test matrix ±5%. Stability better than ±2%. Record at 1 Hz with accuracy ±0.5%. Viscous Dissipation Experiments, $\lvert\omega_i + \omega_o\rvert \le 2\% \lvert\omega_o\rvert$. Viscous Drag Experiments, ω_i error < ± 2%, counterclockwise, ω_o=0. Conductive, non-magnetic, hard: $e_W - (\pi/2)\mu_W > 0.6$. Maintain internal gas bypass rate in the viscous drag experiments: assuming that a small clearance gap between stationary and moving boundaries, maintain $\sum \frac{\ell_i^{\,3}}{L_i} \le 0.004\ \mathrm{mm}^2$, where ℓ_I is the gap thickness of path (i) in mm and L_i is the length of the bypass path in mm. Inscribe marks on selected inner and outer boundary bumps such that one (and only one) mark on each boundary can be seen in the field of view of camera B at any given time. The marks should be straight and aligned with the radial direction. Their edges should be sharp; their width should be imaged on at least 5 pixels and at most 20 pixels. Their length in the radial direction should span the distance between center and crest of the boundary bump on which they are inscribed.
Top plates and windows	5.2.5	Asperities $\le 10\lambda_g$; $e_W \ge 0.75$, $\mu_W \le 0.20$; conductive, non-magnetic; coating resistivity of windows on the flow side ≤ 2000 ohm/square. Windows should permit observations of the spheres and the gas flow using camera B at locations shown in Table 4 (±2°) and should allow a rectangular field of view defined in 5.6. Provide samples of windows and plates no smaller than 4x4 cm^2 to Cornell for impact testing and approval.

Flat base	5.2.6	Asperities $\leq 10\lambda_g$; $e_W \geq 0.8$, $\mu_W \leq 0.15$. Conductive, non-magnetic. Provide a sample no smaller than 4x4 cm^2 to Cornell for impact testing and approval. <u>For the Viscous Drag Experiments</u>: Distributors: arrays of holes $\leq d/2$ spanning at least 80% of the entire width, no longer than 5d in the flow direction, with pressure drop $\geq 2\ \Delta p_g$, at positions shown in Table 3. Static pressure taps: (d/4) diameter holes at positions shown in Table 3 (±2°). Adjust line response time (see 5.9).
Gases	5.2.7	Molecular weight: 28±2 g/mole; viscosity at STP: $1.8\ 10^{-5}$ kg/m.s ± 10%. Provide actual gas composition.
Manifold	5.2.8	For the Viscous Drag Experiments: Provide gas flow rates shown in the test matrix. Mass flow controller to D_1 and D_2 with relative accuracy better than $\pm\Delta Q/Q$ shown in the test matrix for the co-flow region. During operations of the "isokinetic" region, maintain the pressure difference across it $(P_{D_1} - P_{D_2}) < (1/20)(45/180)(P_{D_1} - P_{D_3})$.
Mean solid volume fraction	5.2.9	Determine/verify flow development by recording the mean solid volume fraction at least at the 10 locations shown in Table 4. Measure the cross-sectional averaged solid volume fraction $\bar{\nu}$ with absolute accuracy better than ±1.5%. Provide at least 90 samples at $\bar{\nu}$ = 10%, 250 at $\bar{\nu}$ = 20%, 630 at $\bar{\nu}$ = 30%, 1490 at $\bar{\nu}$ = 40%, 2980 at $\bar{\nu}$ = 50% and 4100 at $\bar{\nu}$ = 55% acquired at a rate no faster than ω.
Spheres	5.3	Non-magnetic, hard, conductive spheres. Asphericity < 1% d. Asperities $\delta < 10\ \lambda_g$. $e_{eff} \sim e - (\pi/2)\mu > 0.7$. Relative error in $\bar{\bar{\nu}} < \pm 1\%\ \bar{\bar{\nu}}$. Know the actual number of spheres in each experiment within ±0.1%. Provide sphere samples to Cornell for impact testing and approval. Samples should have a diameter in the range 2.5 mm$\leq d_{sample} \leq$3.5 mm.
Atmosphere	5.4	Absolute pressure and temperature recorded to ± 2% at a minimum rate of ω/10. Absolute temperature steady to within ±1.5% and in the range 285°K to 300°K. Absolute cell pressure steady to within ±1.5%.
Microgravity	5.5	Maximum quasisteady acceleration, see test matrix. Maximum rms accelerations: $\max(g_{rms}/2\pi f) \leq \sqrt{T}$, see test matrix. Ignore data for θ_{ss} following a transient, see test matrix. Measure accelerations along three axes at a rate ≥ 400 Hz.

Cameras	5.6	Camera A: Standard digital video, image the entire cell and download to ground. Camera B: Can be positioned at least over the 10 locations shown in Table 4. Field of view: The camera should be oriented to take "portrait" images with long axis spanning the distance between the two moving boundaries; it should visualize the flow between the center of bumps on the inner moving boundary and the center of bumps on the moving outer boundary. Field of focus within $d/2 \leq z \leq 3d/2$ from the window. motion and focus blur < 2 pixels. Resolution: $N_y \geq 45\ Y/d$, $N_x \geq 8.5\ N_y\ d/Y$. measurement of sphere velocities: $t_{shutter} < 2\ Y/N_y\ U_{max}$. Minimum frame rate F_{min}; minimum number of images N_{min} (Eq. 59), see test matrix. Actual number of images, $N_{actual} \geq N_{min}\ (F/F_{min})$.
Lighting	5.7	Sufficient to detect spheres using the vision algorithm without image saturation; use a ring light with distortion of circle on image < 20% across field of view.
Mean gas volume flow rate	5.8.2	Measure the mean gas volume flow rate in the co-flow and counter flow regions within the precision shown in the test matrix, which is consistent with a relative error in $R_{drag} < \pm 14\%$.
Gas pressure	5.9	Local gradient measured with uncertainty < ±2%; acquisition frequency $\omega/10$; response tuned to satisfy $1/\pi\ \omega_{min} \leq \tau \leq \theta_{ss_{min}}$.

Table 3 - angular positions of distributors and pressure taps through the channel base

θ is measured clockwise from the inlet distributor D_1

hole	D_1	D_2*	D_3	P_1	P_2	P_3	P_4	P_5	P_6	P_7	P_8	P_9
θ (°)	0	45	180	5.625	39.375	78.75	112.5	146.25	216	252	288	324

* Distributor D2 is only used if the mean gas volume flow rate is inferred isokinetically from solid velocities and volume fraction.

Table 4 - angular positions of window centers

θ is measured clockwise from the inlet distributor D_1

window	W_1	W_2	W_3	W_4	W_5	W_6	W_7	W_8	W_9	W_{10}
θ (°)	22.5	61.875	95.625	129.375	163.125	198	234	270	306	342

NOMENCLATURE

a_t	Student's t-distribution parameter
A_f	exposed filter cross-section area
A_{void}	cross-section of void between stationary & moving walls

b_s	boundary granular energy flux coefficient
B_1, B_2, B_3	coefficients in Eq. (49)
c	coefficient in Eq. (73)
C, C_0	capacitances
d	flow sphere diameter
d_i	inner boundary bump diameter
d_t	line diameter leading to a pressure transducer
$D_{inelastic}$	volumetric rate of collisional dissipation
d_o	outer boundary bump diameter
d_{sensor}	capacitance sensor diameter
d_{tracer}	tracer diameter
$D_{viscous}$	volumetric rate of viscous dissipation
E	Young's modulus
e	coefficient of normal restitution
E^*	$E/2(1-\sigma^2)$
E_{CCD}	minimum detectable emissivity
e_{eff}	effective coefficient of restitution
e_t	tolerated error from the vision algorithm
e_w	wall normal restitution
F	camera frame rate for granular tracking
F_{min}	minimum acceptable camera frame rate
f	vibrational frequency, capacitance amplifier frequency
$F_{\#}$	lens F-stop
f_{-3dB}	-3dB cut-off frequency
F_{drag}	volumetric drag force
Fr_{eff}	Froude number based on g_{eff}
Fr_i	Froude number in the direction i
F_{simul}	virtual frame rate in numerical simulations
f_s	boundary granular stress coefficient
F_{tracer}	camera frame rate for tracer measurements
$G(\nu)$	$\nu\, g_{12}(\nu)$
$g_{12}(\nu)$	Carnahan and Starling pair distribution function
g_{eff}	effective acceleration
g_i	gravitational acceleration vector
g_{rms}	rms vibrational acceleration
h_c	limiting interstitial gap (Eq. 19)
h_d	limiting interstitial gap (Eq. 20)
h, h_-, h_+	functions in Eqs. (50) and (51)
$k_1(\nu)$	Eq. (15)
$k_2(\nu)$	Eq. (14)
K_e	effective dielectric constant
K_h	dielectric constant of the host fluid; in air, $K_h = 1$
Kn_g	gas Knudsen number (Eq. 32)
Kn_s	solid Knudsen number (Eq. 36)

K_p	material dielectric constant of the flow spheres
L	race track cell straight section length
ℓ	characteristic length of the capacitance probe
ℓ_i	thickness of an internal gas bypass path
ℓ_{eq}	equivalent thickness of the internal gas bypass paths
L_i	length of an internal gas bypass path
L_{eq}	equivalent length of the internal gas bypass paths
ℓ_t	length of line connected a pressure transducer
ℓ_s	boundary coefficient (Eq. 62)
M	lens magnification
N_1, N_2	integers
N_{actual}	actual number of images for granular tracking (Eq. 59)
N	number of voids between stationary & moving walls
n_i	normal unit vector
N_{images}	number of images for gas velocity measurement
N_{min}	minimum number of images for granular tracking (Eq. 58)
n_{tracer}	number of tracers in a strip
N_x	number of pixels in the x-direction
N_y	number of pixels in the y-direction
p	pixel size on the CCD
p'	spatial resolution on the CCD with sub-pixel tracking accuracy
P_{coll}	volumetric rate of collisional production
p_g	gas static pressure
P	filter permeability coefficient ($kg/m^2.s$)
p_{D_1}	pressure at distributor D_1
P_{laser}	laser power
P_{rel}	volumetric rate of viscous production
p_s	granular pressure
P_{void}	cross-sectional perimeter of void between stationary & moving walls
q_i	granular fluctuation energy flux
Q_1, Q_2, Q_3	gas volume flow rates (vfr) through distributors D_1, D_2 and D_3
Q_{g1}, Q_{g2}, Q_{g3}	gas vfr through the co-flow, counter-flow and isokinetic regions
Q_{void}	gas flow rate through voids between stationary & moving walls $Q_{void} \sim N\,[A^3_{void}/P^2_{void}]\,\lvert dp/\bar{R}\,d\theta\rvert/2\mu_g$
Q_{rel}	gas volume flow rate relative to the solid velocity $Q_{rel} \sim \lvert ug\text{-}us\rvert\bar{v}\ YZ \sim [Y\,Z\,d^2/18\mu_g\bar{v}\ Rdrag]\,\lvert dp/\bar{R}\,d\theta\rvert$
$\tilde{Q}_{g3}$	estimator of gas flow rate in the isokinetic section
Q_f	gas vfr across a filter
Q_{bypass}	internal gas bypass vfr
Q_{test}	gas vfr in an internal gas bypass test
r, θ, z	cylindrical coordinates

$\bar{R}$	mean radius ≡ $(R_o+R_i)/2$
R_{diss}	viscous dissipation coefficient
R_{drag}	drag coefficient
Re	Reynolds number based on shear rate ≡ $\rho_g\gamma d^2/\mu_g$
Re_{rel}	Reynolds number based on gas-solid relative velocity
Re_T	Reynolds number based on $\sqrt{T}$
R_i	cell radius to inner boundary bump centers
R_o	cell radius to outer boundary bump centers
R_τ	dimensionless gas pressure gradient (Eq. 23)
s	curvilinear distance
S^*	viscous production coefficient
$\hat{S}_{ij}$	deviatoric part of S_{ij}
S_{ij}	rate of strain tensor
St	Stokes number (generic)
$\bar{St}$	mean Stokes number ≡ $\theta_s\,\Delta U/Y'$
St_c	critical Stokes number for nearly Maxwellian distribution (Eq. 28)
St_{local}	local Stokes number (Eq. 26)
St_{rel}	Stokes number based on gas-solid relative velocity
T	granular temperature
$T_{\theta\theta}$	granular temperature in the flow direction
T_{rr}	granular temperature across the moving boundaries
t	time
t_i	tangent unit vector
T_{bs}	beam splitter transmission
$T_{m_i}(j)$	mass weighted granular temperature of species j in i-direction
t_{sh0}	shutter opening time (manufacturer specification)
$t_{shutter}$	shutter opening time
U	boundary velocity
u_g	gas velocity in the flow direction
$u_{g,max}$	maximum detectable tracer velocity
U_i, U_o	linear velocities of the inner and outer boundaries
U_{max}	$= \max(U_i,U_o)$
u_s	granular velocity in the flow direction
$u_s{'}_i$	granular fluctuation velocity vector
u_{s0}, u_{s1}	granular velocity at the two moving boundaries
u_{scrit}	critical impact velocity (Eq. 76)
$\tilde{u}_s(r)$	estimator of the mean solid velocity
v, V, V_0	voltages
V_{rel}	mean relative gas-solid velocity
v_s	granular velocity in the transverse direction
V_1,V_2	volumes on two sides of a differential pressure transducer
x, y, z	cartesian coordinates (Fig. 8)

x_i	coordinate direction i
Y	distance separating the centers of two opposite boundary bumps
y_m	height of the capacitance probe measurement volume, see Fig. 17
Y'	interior sphere center separation = Y - $(d_o+d_i)/2$ - d
Z	distance between flat side walls
Z_a	impedance

<u>Greek</u>

β	$\equiv 18\mu_g\nu(1-\nu)^2 R_{drag}(\nu)/d^2$
β_0	coefficient of tangential restitution
δ	asperity size
$\delta_{0.99}$	gas boundary layer thickness
δ_{ij}	Kronecker delta
ε_m	dimensionless lubrication cut-off (Eq. 16)
ε_0	permittivity of free space = 8.854 10^{-12} F/m
γ	shear rate
η	granular shear viscosity (Eq. 5)
η_{fl}	tracer fluorescent efficiency
κ	granular bulk viscosity (Eq. 4)
λ_g	gas molecular mean free path
λ_s	granular mean free path (Eq. 33)
ν	solid volume fraction
$\bar{\nu}$	ν averaged at a cell cross-section
$\bar{\bar{\nu}}$, ν_{ave}	ν over the entire cell
ν_{FD1}, ν_{FD2}, ν_{FD3}	fully-dev. ν in the co-flow, counter-flow and isokinetic regions
ν_c	critical volume fraction for multiple solutions
$\tilde{\nu}$	estimator of the mean solid volume fraction
Θ	estimated experiment duration (Eqs. 94 to 96)
θ	circumferential angle
θ_b	bumpiness coefficient
θ_s	Stokes relaxation time
θ_{ss}	time to steady-state
θ_μ	required duration of microgravity
ρ_g	gas density
ρ_s	solid material density
σ	Poisson's ratio
σ_c	compressive yield strength
τ	transducer response time
τ_g, τ_{gij}	gas shear stress
τ_s, τ_{sij}	granular shear stress
τ_{s0}, τ_{s1}	granular shear stresses at the two moving boundaries
ω	granular collision frequency
ω_i	inner boundary angular velocity

ω_o	outer boundary angular velocity
ξ_s	granular boundary slip velocity
ψ	intrinsic granular property
μ	coefficient of friction (binary impacts)
μ_g	gas viscosity
μ_w	wall friction coefficient
Δ_i	gap separating cylindrical bumps of the inner boundary
Δ_o	gap separating cylindrical bumps of the outer boundary
$\Delta\theta$	angular distributor separation
Δp_g	gas pressure loss
Δp_{test}	gas pressure drop in internal gas bypass tests
$\Delta Q/Q$	prescribed maximum relative error in mean gas volume flow rate
ΔU	boundary relative velocity = $U_i - U_o$
Δu_g^{max}	maximum allowed error in the gas velocity measurement
$\Delta u_{sc}^{\dagger}$	additional granular centerline velocity (Eq. 76)
$\Delta u_s^{\dagger}$	additional granular velocity (Eq. 79)
$\Delta \xi_s^{\dagger}$	additional granular boundary slip velocity (Eq. 78)

Superscripts

$\dagger$	dimensionless quantity